Age-Related Alterations in the Retinal Microvasculature, Microcirculation, and Microstructure

Yantao Wei,[1,2] Hong Jiang,[2,3] Yingying Shi,[2] Dongyi Qu,[2] Giovanni Gregori,[2] Fang Zheng,[2] Tatjana Rundek,[3] and Jianhua Wang[2]

[1]State Key Laboratory of Ophthalmology, Zhongshan Ophthalmic Center, Sun Yat-sen University, Guangzhou, China
[2]Bascom Palmer Eye Institute, University of Miami Miller School of Medicine, Miami, Florida, United States
[3]Department of Neurology, University of Miami Miller School of Medicine, Miami, Florida, United States

Correspondence: Jianhua Wang, Bascom Palmer Eye Institute, University of Miami, Miller School of Medicine, 1638 NW 10th Avenue, McKnight Building - Room 202A, Miami, FL 33136, USA; jwang3@med.miami.edu.

Submitted: January 10, 2017
Accepted: June 21, 2017

Citation: Wei Y, Jiang H, Shi Y, et al. Age-related alterations in the retinal microvasculature, microcirculation, and microstructure. *Invest Ophthalmol Vis Sci*. 2017;58:3804–3817. DOI: 10.1167/iovs.17-21460

Purpose. To characterize age-related alterations in the retinal microcirculation, microvascular network, and microstructure in healthy subjects.

Methods. Seventy-four healthy subjects aged from 18 to 82 years were recruited and divided into four age groups (G1 with age <35 years, G2 with age 35 ~ 49 years, G3 with age 50 ~ 64 years, and G4 with age ≥65 years). Custom ultra-high resolution optical coherence tomography (UHR-OCT) was used to acquire six intraretinal layers of the macula. OCT angiography (OCTA) was used to image the retinal microvascular network. The retinal blood flow velocity (BFV) was measured using a Retinal Function Imager (RFI).

Results. Compared to G1, G2 had significant thinning of the retinal nerve fiber layer (RNFL) ($P < 0.05$), while G3 had thinning of the RNFL and ganglion cell and inner plexiform layer (GCIPL) ($P < 0.05$), in addition to thickening of the outer plexiform layer (OPL) and photoreceptor layer (PR) ($P < 0.05$). G4 had loss in retinal vessel density, thinning in RNFL and GCIPL, and decrease in venular BFV, in addition to thickening of the OPL and PR ($P < 0.05$). Age was negatively related to retinal vessel densities, the inner retinal layers, and venular BFV ($P < 0.05$). By contrast, age was positively related to OPL and PR ($P < 0.05$).

Conclusions. During aging, decreases in retinal vessel density, inner retinal layer thickness, and venular BFV were evident and impacted each other as observed by simultaneous changes in multiple retinal components.

Keywords: age, retina, microcirculation, microvasculature, microstructure

The retina is an extension of the brain and comprised of neural cells. The neural network in the retina forms an organized and stratified structure with neurons interconnected by synapses that sense light and process images. As the highest oxygen-consuming tissue, the retina develops a unique vascular system with a blood supply to match its metabolic demand.[1] Like other human organs, changes in the retinal vascular system occur during normal aging and are also secondary to onset and progression of ocular and systemic diseases, such as diabetes, hypertension, and multiple sclerosis.[2–4]

Owing to the transparency of the ocular media, the retinal microstructure, microvascular network, and microcirculation can be directly observed and measured, which facilitates the monitoring of age-related changes. Retinal changes may also reflect the aging process in other organs, such as the brain. Studying retinal vascular and structural changes across normal aging will provide insightful information for better understanding of both physiological and pathophysiological mechanisms of ocular, cerebral, and systemic diseases.

Retinal neurodegeneration presented as thinning of the retinal nerve fiber layer (RNFL) and ganglion cell layer (GCL) during aging has been well-documented since the use of optical coherence tomography (OCT) approximately 20 years ago.[5–7] Retinal microcirculation is reported to decrease across age, mainly in the retinal venules.[8] However, with the recent advances in OCT angiography (OCTA), there are controversial reports of age-related changes in the retinal microvascular network.[9–11] The goal of this study was to characterize age-related alterations of retinal microcirculation, microvasculature, and microstructure in healthy subjects.

Methods

Subjects

All participants were healthy subjects without any ocular pathology, previous ocular trauma, or surgery. Exclusion criteria were refractive error greater than ±6 diopters, obvious media opacity, and poorly dilated pupils obscuring clear visualization of the retina. Subjects who had any systemic disease, such as uncontrolled diabetes or hypertension, were also excluded. The protocol conformed to the Declaration of Helsinki. The study was approved by the institutional review board of the University of Miami Miller School of Medicine. Written informed consent was obtained from all participants.

The subjects were divided into four groups in intervals of 15 years. Group 1 (G1) was aged <35 years, Group 2 (G2) was aged from 35 to 49 years, Group 3 (G3) was aged from 50 to 64 years, and Group 4 (G4) was aged ≥65 years. All subjects underwent comprehensive ophthalmic examinations including

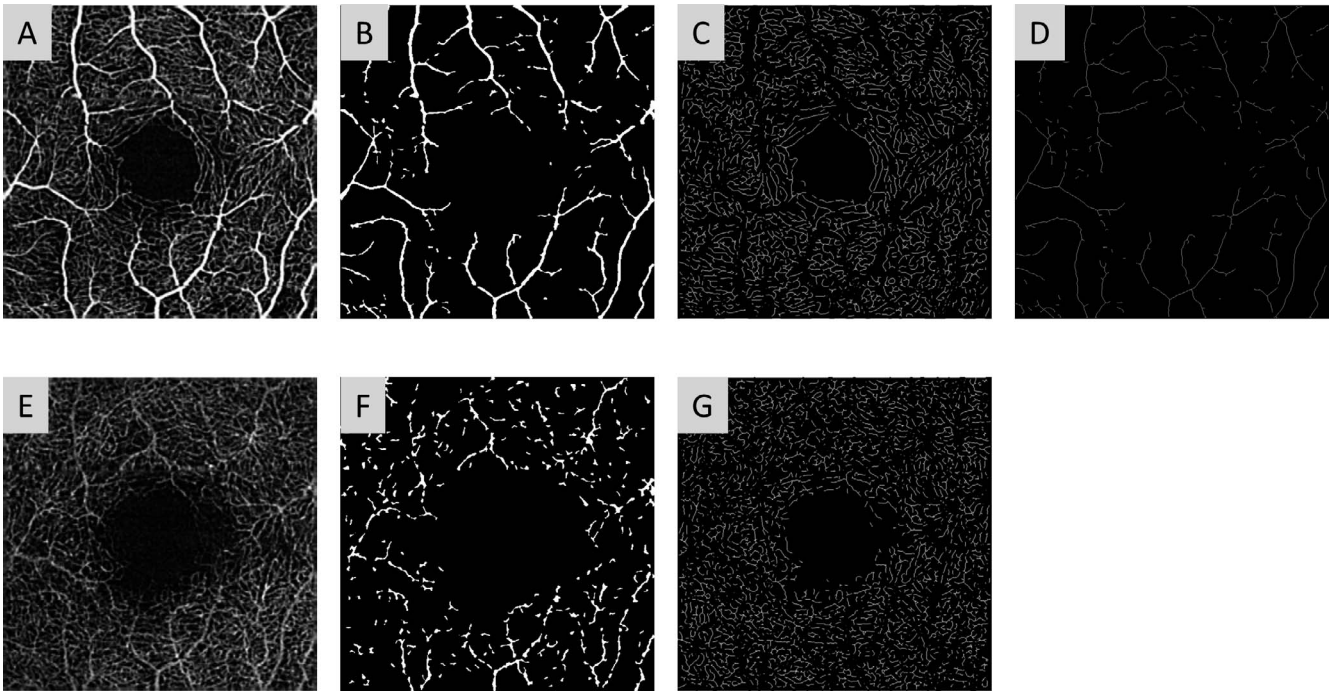

Figure 1. Image processing and separation of large and small vessels. The raw OCTA enface view image of the SVP (**A**) with a field of view 3×3 mm^2 was processed to extract the large vessels with a diameter $> \sim$25 μm (**B**). Both the small vessels (**C**) and large vessels (**D**) were skeletonized for fractal analyses. For the DVP (**E**), the shadowgraphic project artifacts (**F**) from the SVP (**A**) were removed. The remaining small vessels were skeletonized (**G**) for analyses.

best corrected visual acuity, manifest refraction, and slit-lamp examination.

Retinal Vessel Density Calculation by OCTA and Fractal Analysis

The retinal vessel network (RVN) images were noninvasively obtained using Zeiss HD-OCT with an Angioplex OCTA device (Carl Zeiss Meditec, Dublin, CA, USA). This system captures depth-encoded retinal vasculature with a scan rate of 68,000 A-scans per second using an optical source centered at a wavelength of 840 nm and a bandwidth of 90 nm.[12] The OCTA images are generated analyzing differences in both intensity and phase information between a number of B-scans acquired at the same locations.[12] In the present study, the 3×3 mm and 6×6 mm scans were acquired for each subject. The 3×3 mm scan pattern consisted of 245 A-scans in each B-scan along the horizontal dimension and 245 B-scans, each repeated four times. The 6×6 mm scan pattern consisted of 350 A-scans in each B-scan and 350 B-scans, each repeated two times. Angiographic images of the total retinal vascular network (RVN), superficial vascular plexus (SVP), and deep vascular plexus (DVP) were exported for further processing and fractal analysis. The SVP refers to the vessel network that spreads laterally in the nerve fiber and ganglion cell layers between the internal limiting membrane (ILM) and the inner plexiform layer (IPL). DVP is the microvascular network located on the surface of the outer nuclear layer (ONL) between the inner nuclear layer (INL) and the outer plexiform layer (OPL).[12]

The OCTA images were resampled to 1024×1024 pixels for vessel segmentation by a custom software program in Matlab (The Mathworks, Inc., Natick, MA, USA).[13,14] This software executed a series of image processing procedures to create a binary image of the vessels, including inverting, equalizing, and removing nonvessel structures and background noise. In the binary image, the large vessels were defined as any vessel with a diameter $\geq$25 μm and were extracted from the OCTA images. The remaining vessels were defined as the small vessels. The large vessels extracted from RVN and SVP were skeletonized and partitioned for fractal analysis. The large vessels in DVP are regarded as the shadowgraphic projection artifacts,[15] and were not analyzed. Similarly, the small vessels of RVN, SVP, and DVP were analyzed (Fig. 1). The foveal avascular zone (FAZ) was detected based on the intensity gradient of the image and was used for quadrantal and annular partition. After excluding FAZ (diameter = 0.6 mm), the annulus from 0.6 to 2.5 mm in diameter was defined as the annular zone with a band width of 0.95 mm in a 3×3 mm^2 angiogram (Fig. 2). Similarly, the annulus from 0.6 to 5.0 mm refers to the annular zone with a bandwidth of 2.2 mm in a 6×6 mm^2 angiogram. Using the fractal analysis toolbox (TruSoft Benoit Pro 2.0, TruSoft International, Inc., St. Petersburg, FL, USA), the box counting method was used to calculate the fractal dimension (Dbox) in the annulus, which represents vessel density in each zone (Fig. 3). In addition, the ratio of the small vessel density to the large vessel density was calculated for each eye.

Retinal Blood Flow Velocity (BFV) Measurement by Retinal Function Imager (RFI)

The RFI (RFI-3000, Optical Imaging, Rehovot, Israel) consists of a standard fundus camera, a stroboscopic flash lamp system, and an advanced digital camera.[16,17] The apparatus has been described in detail in a previous publication. Hemoglobin was used as a natural, high-contrast chromophore (wavelengths between 530 and 590 nm) to track the erythrocyte moving. For the BFV operating mode, a green ("red-free") interference filter was used with transmission centered at 548 nm at a bandwidth of 17 nm. The BFV was calculated by quantifying the motion of erythrocytes in eight consecutive fundus images typically

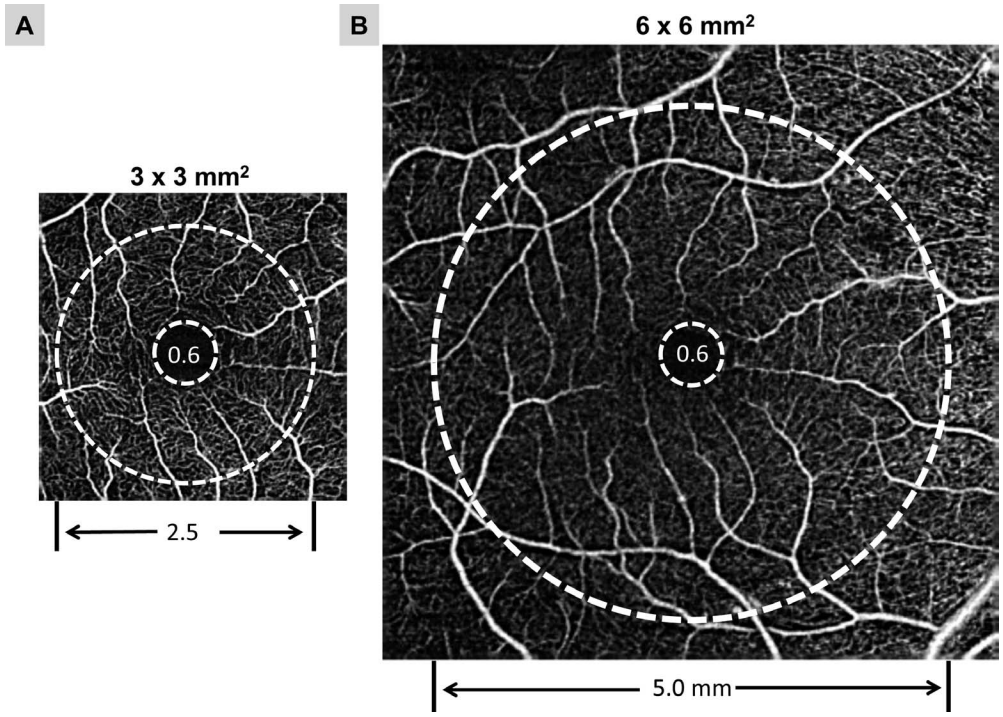

Figure 2. Annulus for quantification of vessel density. The annular zone (0.6–2.5 mm) of the 3×3 mm^2 OCTA enface image (**A**) and the annulus (0.6–5.0 mm) of the 6×6 mm^2 OCTA enface image (**B**) were used for fractal analysis.

generated at an interflash interval of less than 20 ms. To neutralize the effect of pulsation, image acquisitions were synchronized with the subject's systolic pulse.

Blood pressure and heart rate were measured before imaging the eye. One eye from each subject was imaged after pupillary dilation with 1% tropicamide. Multiple image sessions were taken by an experienced photographer. During each session, at least five serial images centered at the fovea were taken at the 35° setting with a calibrated field of view of 7.3×7.3 mm^2. The RFI's built-in software was used to

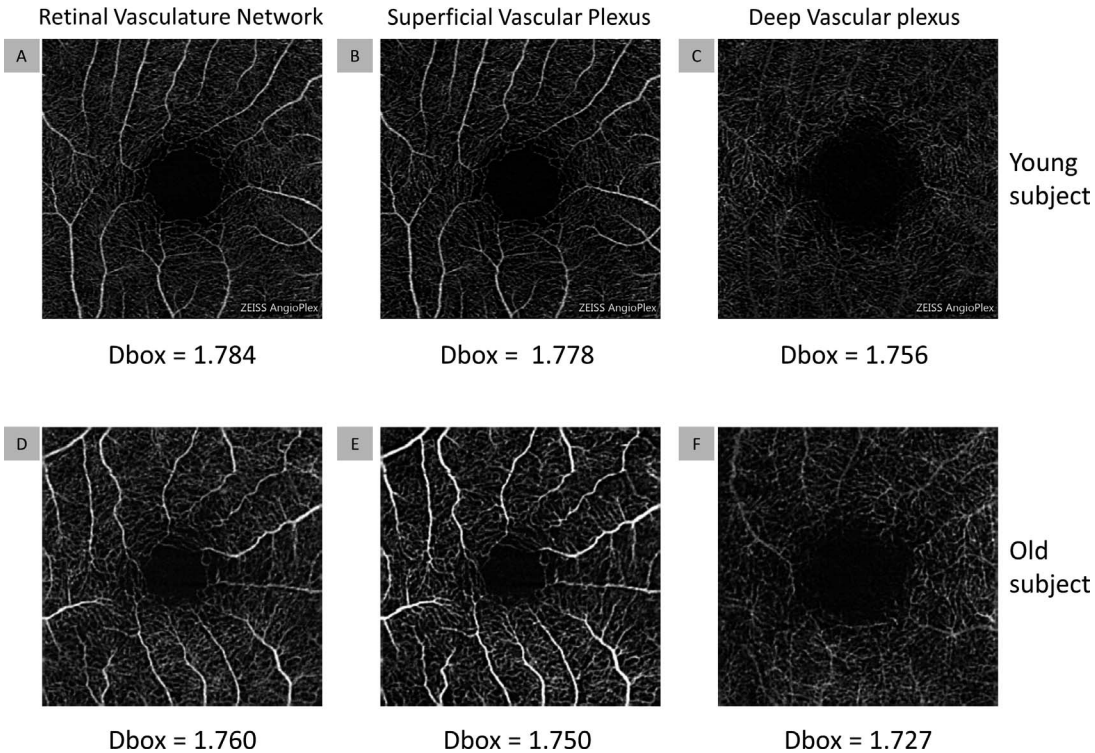

Figure 3. The RVN from 3×3 mm^2 OCTA scans. **A–C** belongs to a 30-year-old subject, while **D–F** belongs to a 69-year-old subject. (**A**, **D**) Total RVN. (**B**, **E**) SVP. (**C**, **F**) DVP.

Investigative Ophthalmology & Visual Science

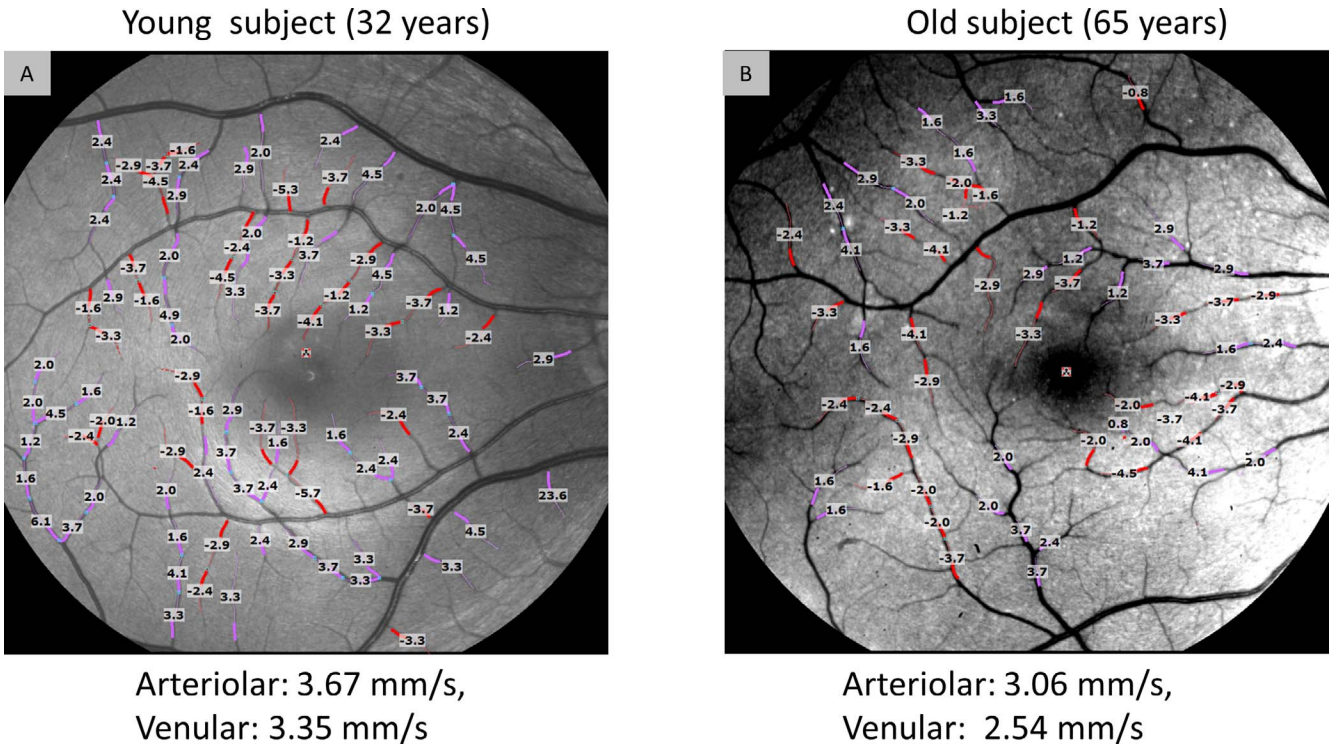

FIGURE 4. Retinal blood flow (RBF) velocity imaged using the RFI. The field of view is 7.3 × 7.3 mm^2. BFV (unit: mm/s) of the secondary and tertiary branches of retinal arteries (*red*) and veins (*purple*) was measured. (**A**) A 32-year-old subject. (**B**) A 65-year-old subject.

analyze arteriolar and venular BFVs. BFV in the secondary and tertiary branches of the retinal vessels was measured (Fig. 4).

Retinal Tomographic Thickness of Intraretinal Layers Measured by Ultra-High Resolution Optical Coherence Tomography (UHR-OCT)

Our custom-built UHR-OCT has been described previously.[18] A super-luminescent diode was used as a light source with a center wavelength of 840 nm and a bandwidth of 100 nm. A spectrometer was adapted with a line scan camera running at 24,000 A-scans per second. To facilitate retinal imaging, a light delivery system with an ocular lens (60 D, Volk Optical, Mentor, OH, USA) was connected to a slit-lamp system. An internal fixation target was generated by a miniature LCD screen. Each patient was imaged using the 512 × 128 macular cube protocol centered on the fovea. This consisted of 128 consecutive B-scans covering an area of 6 × 6 mm^2. Each A-scan contained 1365 pixels and B-scan contained 512 A-scans. The entire raster scanning was acquired in approximately 2.7 seconds with an axial resolution of ~3 μm.

Automatic retinal segmentation software (Orion, Voxeleron LLC, Pleasanton, CA, USA) was used to segment and process the thickness maps of the intraretinal layers with hemispheric and the Early Treatment Diabetic Retinopathy Study (ETDRS) partitions.[18] The macular cube was automatically segmented (Fig. 5) to obtain the total retinal thickness (TRT) and six intraretinal maps, including the RNFL, GCIPL (GCL + IPL), INL, OPL, ONL, and photoreceptor complex (PR).

Statistical Analysis

Statistical analyses were performed using a statistical software package (STATISTICA, StatSoft, Inc., Tulsa, OK, USA). Pearson correlation coefficients were used to determine the associations between age and OCTA, UHR-OCT, and RFI parameters. This model was also used to analyze correlations for each pair of parameters. One-way analysis of variance (ANOVA) was used to test the differences among groups and Fisher post hoc tests were performed to test pair-wise differences among groups. All data were presented as the mean ± SD, and a *P*-value of less than 0.05 was considered statistically significant.

Results

We analyzed 74 healthy subjects, and demographic information of four subgroups is listed in Table 1. Compared to G1, G2 showed significant thinning of the RNFL (Table 2; Fig. 6; $P < 0.05$). G3 showed significant thinning of the RNFL and GCIPL ($P < 0.05$), in addition to thickening of the PR ($P < 0.05$). Interestingly, G3 showed an increase in arteriolar BFV ($P < 0.05$). G4 showed significant losses of the small vessel density in the retina, the superficial and DVPs in both fields of 3 and 6 mm (Fig. 7), and thinning in the TRT, RNFL, and GCIPL, in addition to thickening of the OPL and PR ($P < 0.05$). There were no significant differences of large vessel densities among groups of both fields of 3 and 6 mm (Fig. 7; $P > 0.05$). However, G4 showed smaller ratios of small and large vessels in comparison to G2 ($P < 0.05$). Finally, G4 showed a significant decrease in venular BFV (Fig. 8; $P < 0.05$).

All subjects were analyzed to determine the relationship among the measurements (Figs. 9–12). Age was negatively related to retinal vessel densities of the retinal microvascular network, the superficial and DVPs, the inner retinal layers, including the RNFL, GCIPL, and INL, and retinal BFV in venules (Figs. 9, 10, 12; Table 3; $P < 0.05$). By contrast, age was positively related to OPL and PR (Fig. 11; $P < 0.05$). Age was

Investigative Ophthalmology & Visual Science

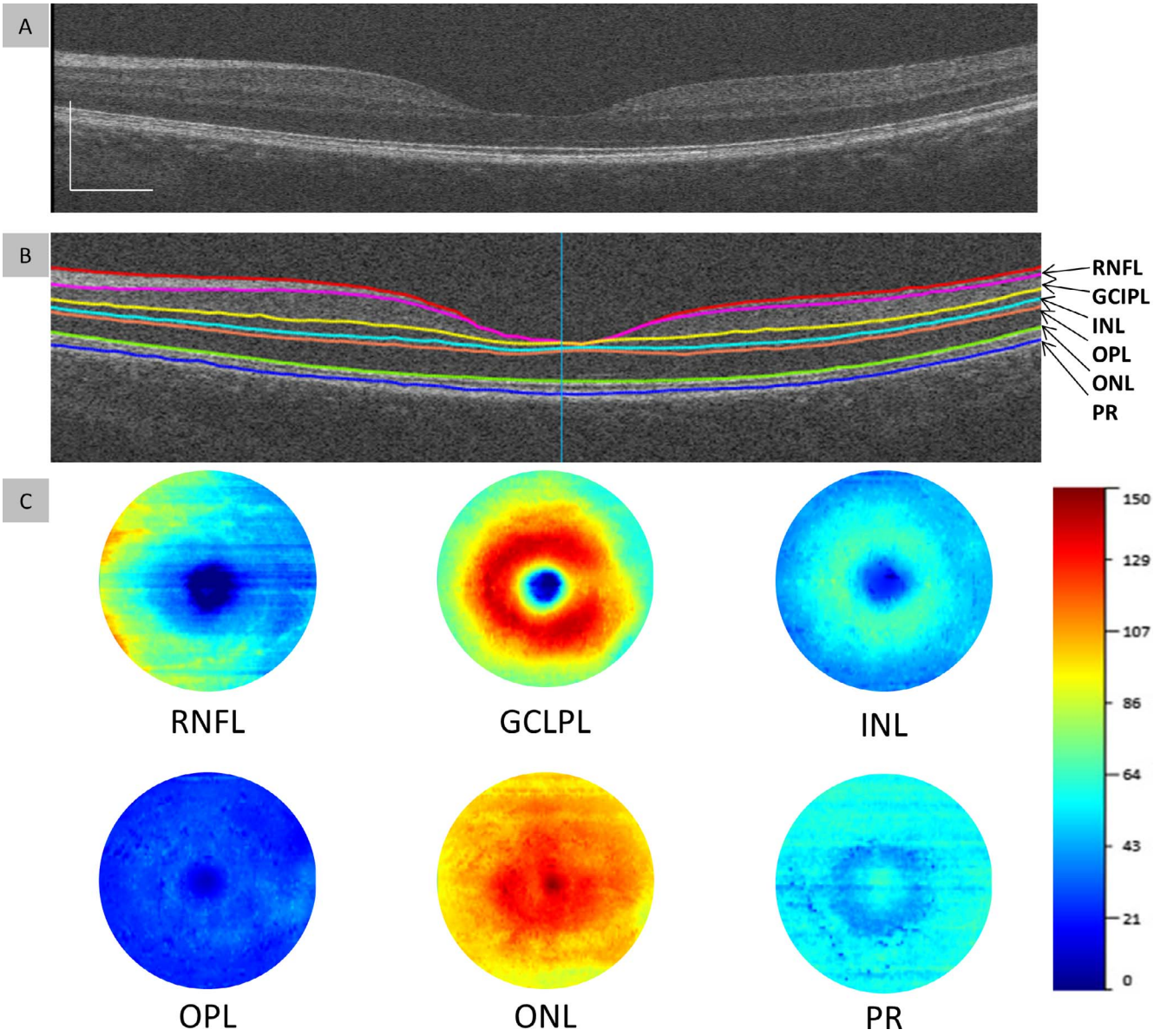

Figure 5. Intraretinal layers and corresponding thickness maps. (**A**) A B-scan. (**B**) Automated segmentation of seven anatomical interfaces. (**C**) Six thickness maps over a disk of 6 mm in diameter obtained from the automated segmentation.

neither related to large vessel densities nor the ratios of small and large vessel densities ($P > 0.05$).

The deep vessel density in the 6-mm field was significantly correlated with the thickness of the TRT, GCIPL, INL, and ONL (Fig. 13; $P < 0.001$). Venular BFV was positively related to the retinal vessel network of the annulus from 0.6 to 5 mm (Fig. 14; $P < 0.05$).

Table 1. Characteristics of the Healthy Subjects

	Mean ± SD	Range
Subject no.	74	
Male vs. female	31:43	
Eye, OD:OS	70:4	
Caucasian vs. Asian vs. Hispanic/Latino	6:36:32	
Age, y	44.4 ± 16.0	18–82
Systolic blood pressure, mm Hg	122.8 ± 16.1	89–164
Diastolic blood pressure, mm Hg	79.2 ± 10.5	59–107
Heart rate (per min)	70.9 ± 10.5	45–92

OD, right eye; OS, left eye.

Discussion

This is the first study to use multiple advanced imaging modalities to determine the microstructural and microvascular alterations of the retina during normal aging. We found that thinning of the RNFL and GCIPL coexisted with the decreased density of the retinal micro-vessels and altered microcirculation during normal aging. Characterizing the microstructure, microvasculature, and microcirculation across a wide range age provided the information about the role of aging on retinal structure and the vascular system. It is critical to analyze these three components in the same group of subjects to better understanding interlinks among them. Previous studies may provide some useful information of one or two components of

Investigative Ophthalmology & Visual Science

Table 2. Measurements of the Retinal Thickness, Vessel Density, and BFV of the Study

Age Groups	Group 1	Group 2	Group 3	Group 4
Range, y	<35	35–49	50–65	>65
Mean ± SD, y	27.2 ± 4.2	40.8 ± 4.2	57.3 ± 4.2	70.4 ± 4.5
Number	24	23	16	11
Retinal thickness, Mean ± SD, μm				
TRT	278.7 ± 11.9	276.0 ± 10.5	274.5 ± 10.2	268.1 ± 8.8*
RNFL	39.2 ± 4.1	37.0 ± 3.2*	35.7 ± 2.9*	33.4 ± 2.9*
GCIPL	70.1 ± 4.2	68.7 ± 3.9	66.0 ± 5.3*	63.4 ± 3.9*
INL	36.4 ± 1.8	36.3 ± 1.8	35.6 ± 1.7	35.2 ± 1.7
OPL	19.7 ± 1.9	19.9 ± 2.1	21.1 ± 2.5	22.3 ± 3.9*
ONL	75.5 ± 3.8	76.2 ± 3.7	75.6 ± 4.3	73.4 ± 4.8
PR	37.7 ± 4.0	38.0 ± 4.2	40.5 ± 3.1*	40.4 ± 2.4*
Vessel density in the annulus from 0.6 to 2.5 mm, Mean ± SD, Dbox				
Retina	1.771 ± 0.013	1.757 ± 0.027	1.759 ± 0.028	1.728 ±0.038*
Superficial	1.759 ± 0.031	1.749 ± 0.026	1.747 ± 0.034	1.720 ± 0.034*
Deep	1.749 ± 0.033	1.735 ± 0.020	1.739 ± 0.022	1.693 ± 0.052*
Vessel density in the annulus from 0.6 to 5.0 mm, Mean ± SD, Dbox				
Retina	1.815 ± 0.013	1.813 ± 0.013	1.809 ± 0.023	1.787 ± 0.035*
Superficial	1.806 ± 0.012	1.796 ± 0.028	1.797 ± 0.035	1.778 ± 0.027*
Deep	1.788 ± 0.042	1.802 ± 0.038	1.789 ± 0.038	1.732 ± 0.047*
BFV, Mean ± SD, mm/s				
Arteriole	3.3 ± 0.7	3.6 ± 0.7	4.0 ± 1.0*	3.2 ± 0.9
Venule	3.0 ± 0.6	2.9 ± 0.5	2.8 ± 0.6	2.6 ± 0.5*

Asterisk (*) denotes $P < 0.05$ compared to G1.

the neuro-vascular-hemodynamic system (Table 4),[8–11,19–26] but not the full picture of age-related alterations and their relations. Better understanding the changes of the system during normal age is essential for understanding disease processing while age plays a role in the change. Most importantly, this study including all three components provided an opportunity to speculate which component changes first during aging. The present study showed that aging played an important role in all three components (i.e., microstructure, microvasculature, and microcirculation) of the neuro-vascular-hemodynamic system, which provides insightful information on normal aging and an important baseline for studying diseased eyes.

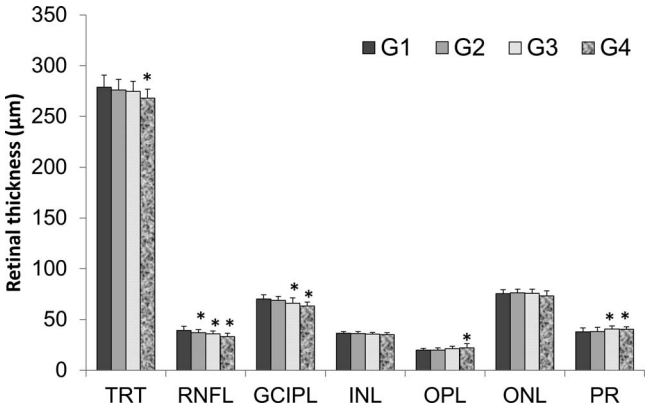

Figure 6. Intraretinal thickness for the different age groups. Compared to G1, G2 showed significant thinning of the RNFL ($P < 0.05$). G3 showed significant thinning of the TRT, RNFL, and GCIPL ($P < 0.05$), in addition to thickening of the PR ($P < 0.05$). G4 showed significant thinning in the RNFL and GCIPL, in addition to thickening of the OPL and PR ($P < 0.05$). *Asterisk* (*) denotes $P < 0.05$ compared to G1. *Bars* = SD.

The retinal structural alterations during aging have been evaluated by OCT.[21,23–26] In previous studies, Harwerth et al.[24] suggested that a period of 70 years of life results in a decrease in RNFL thickness of 15%, a loss of axons of 50%, and a 40% reduction in axon density in the RNFL. Longitudinal analyses showed ganglion cells measured as GCC thickness decreased 0.25 μm per year, whereas the RNFL thickness decreased 0.14 μm per year with age over 40 years. The cross-sectional analyses showed the GCC thickness was 0.17 μm thinner per year, whereas the RNFL was 0.21 μm thinner.[26] Two previous studies of aging effects using Scanning Laser Polarimetry reported significant declines of 0.14 to 0.25%/year in RNFL thickness during a life span of 60 years.[27,28] In the present study, up to six intraretinal layers were delineated and measured with good repeatability using our custom-made ultra-high resolution OCT and the Orion automatic segmentation software. Our findings showed that the thinning occurred mainly within the inner layers of the retina, which consist of ganglion cells and their nerve fibers. Consistent with published results, the present study revealed prominent thinning of 0.35% (0.13 μm) per year in RNFL thickness and 0.21% (0.14 μm) per year in GCIPL thickness during a period of six decades.

In contrast to the thinning of the inner layers of the retina, there was aging-related thickening found in the sublayers of the outer retina, including the OPL and PR layer in this study. Histologically, the density of the cone and RPE cells showed no significant loss in the fovea of donor eyes during the seven decades of life.[29] Ooto et al.[30] found thinning of the inner segment, thickening of the outer segment, and no change in the OPL with increasing age. These findings are supported by immunohistochemical assays. Using oxygen microelectrodes, the outer segments of the photoreceptors were determined to be the most metabolically active layer in the retina.[31,32] Therefore, instead of the cell density, the PR thickness may depend on its metabolic and functional change with increasing age, which are closely related to the RPE function or choroidal

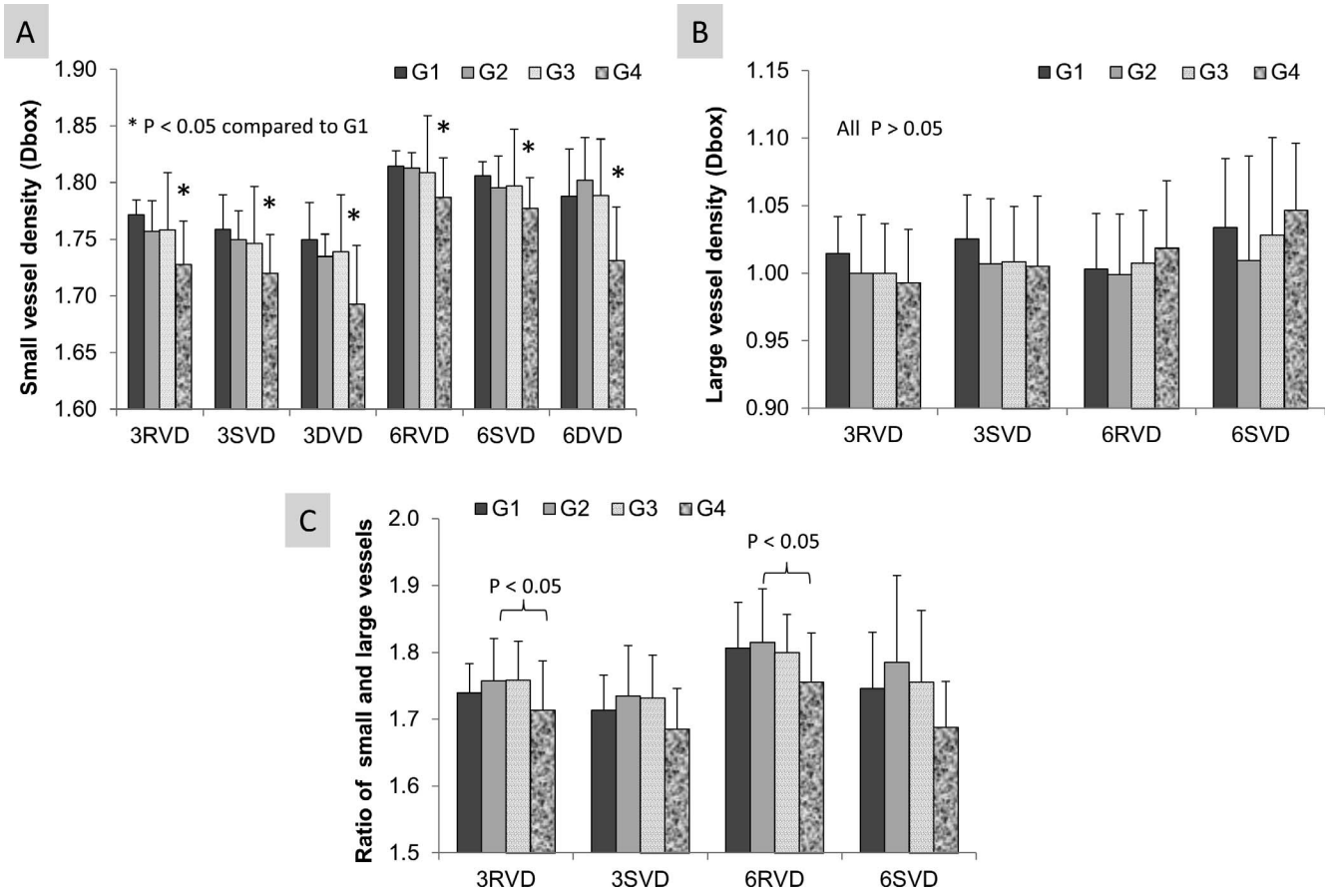

Figure 7. Retinal microvascular densities for the different age groups. Compared to G1, G4 showed significantly lesser small vessels in the RVN, the SVP and DVP in both annuli from 0.6 to 2.5 mm and 0.6 to 5.0 mm (**A**, $P < 0.05$). There were no significant differences of the large vessels among groups in both RVN and SVP in both annuli (**B**, $P > 0.05$). The ratios of the small vessel density to the large vessel density were significantly smaller in G4 compared to G2 in both annuli (**C**, $P < 0.05$). Note the large vessels extracted from the DVP are regarded as the shadowgraphic project artifacts; therefore, the density was not measured. 3RVD, total retinal vessel density in the annulus from 0.6 to 2.5 mm; 3SVD, superficial vessel density in the annulus from 0.6 to 2.5 mm; 3DVD, deep vessel density in the annulus from 0.6 to 2.5 mm; 6RVD, total retinal vessel density in the annulus from 0.6 to 5.0 mm; 6SVD, superficial vessel density in the annulus from 0.6 to 5.0 mm; 6DVD, deep vessel density in the annulus from 0.6 to 5.0 mm. *Asterisk* (*) denotes $P < 0.05$ compared to G1. *Bars* = SD.

circulation. Maruko et al.[33] reported that the thickness of the outer retina did not decline with the age-dependent thinning of the choroid in the fovea. Using OCT, the retinal pigment epithelium–Bruch's membrane (RPE-BM) thickness was found to be positively correlated with age in normal subjects.[34] In addition, structural changes in RPE-BM have been revealed in histopathological studies, including calcification, loss of melanin granules, and accumulation of residual bodies.[35,36] Therefore, it is assumed that decreased phagocytosis in RPE might be the underlying mechanism attributed to the thickening of the PR in the fovea during aging.

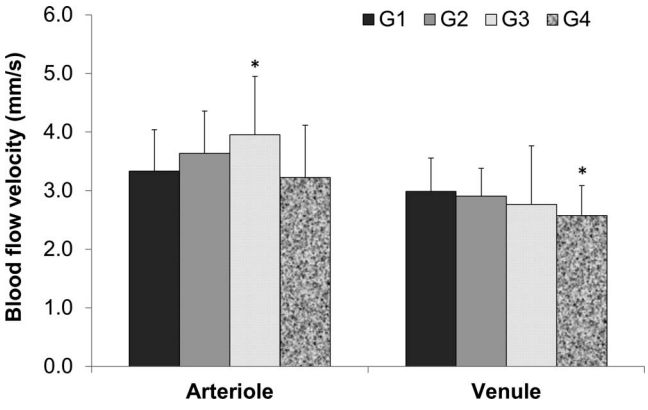

Figure 8. Retinal BFV for the different age groups. G3 showed an increase in arteriolar BFV ($P < 0.05$) compared to G1. G4 showed a significant decrease in venular BFV ($P < 0.05$). *Asterisk* (*) denotes $P < 0.05$ compared to G1. *Bars* = SD.

As the inner retinal layers thin across aging, retinal vessels in the inner layers alter as well. However, recent studies of retinal vasculature using OCTA reported controversial results. There is no consensus on whether aging plays a role in the changes of the inner retinal vasculature. As an organized, multilayered stratified tissue, the human retina possesses two horizontal vascular layers, the SVP and DVP. Using OCTA scanning and fractal analysis in 52 Indian eyes (age 20–67 years), Gadde et al.[11] found that the vessel density was greater in the DVP than the SVP, whereas the vessel density in all the parafoveal sectors was unaffected by age. By contrast, Yu et al.[9] measured the mean vessel density in 45 Chinese subjects (age 24–59 years) and found that vessel density was decreased annually by 0.4% and significantly correlated with age. Interestingly, Yu et al.[10] later found the relation between macular vessel density and age did not exist with a relatively large sample (64 subjects, age 20–62 years). Compared to these

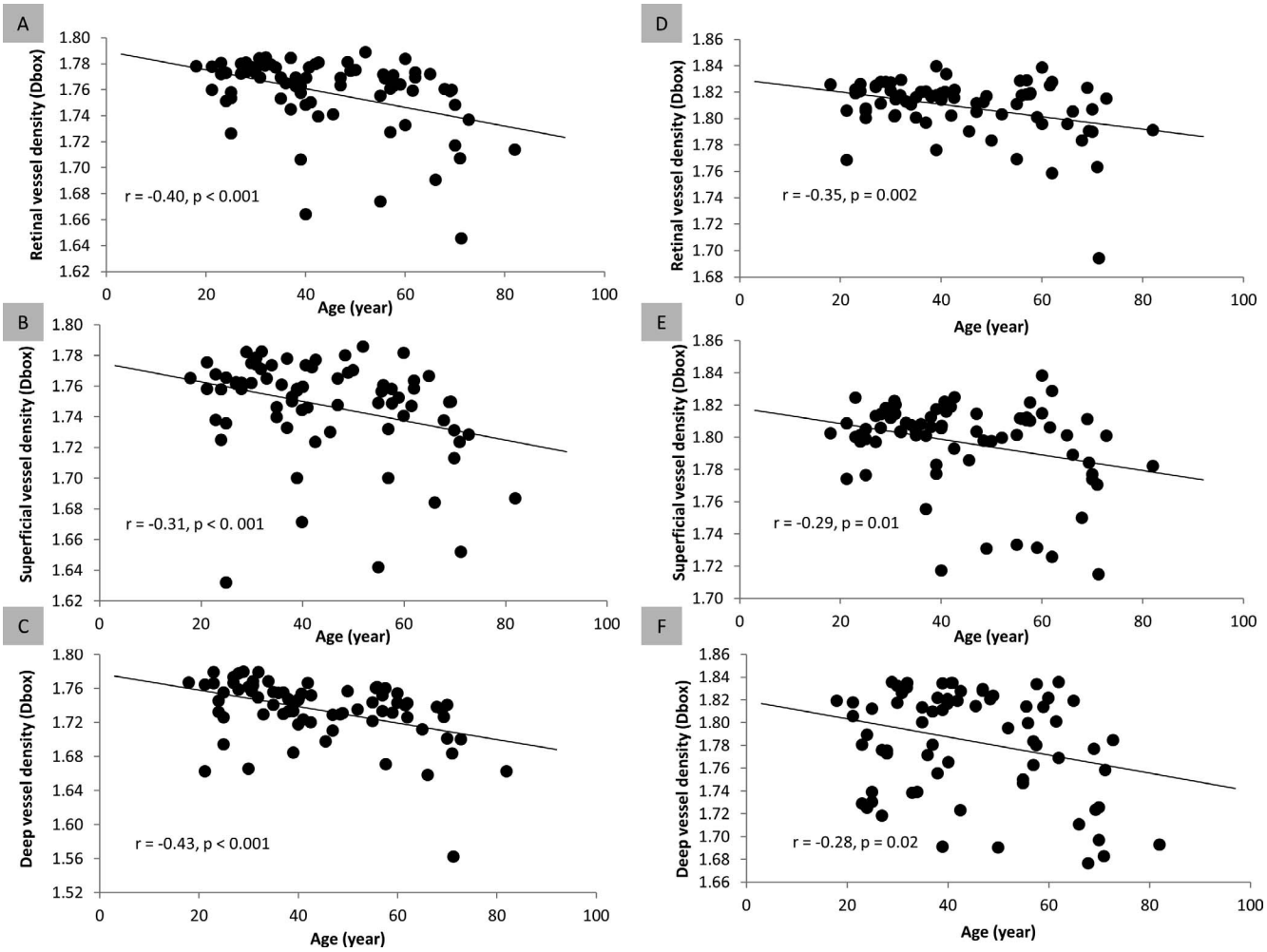

Figure 9. Relationship between age and retinal vessel density. (**A**, **D**) Total retinal vessel density. (**B**, **E**) Superficial retinal vessel density. (**C**, **F**) Deep retinal vessel density. The plots on the *left* (**A**–**C**) correspond to an annulus from 0.6 to 2.5 mm in the perifoveal region. The plots on the *right* (**D**–**F**) correspond to an annulus from 0.6 to 5 mm in the perifoveal region.

previous studies, the present study had a wider age range and larger sample size, and used fractal analysis that has been previously validated for image processing. In the current study, small vessels and large vessels were analyzed separately and the shadowgraphic projection artifacts were removed from the DVP. These modifications for detailed image analysis may contribute to the detection of the age effect on microvasculature in the inner retinal layers. Our results clearly showed that age was a factor related to the decreased micro-vessel density in the DVP and SVP measured in both fields of 3×3 mm^2 and 6×6 mm^2 centered on the fovea, with a decline of 0.3% per decade in SVP and 0.5% to 0.6% per decade in DVP during a life span of 60 years.

The angiography of RVN theoretically includes all vascular networks in both SVP and DVP. However, the enface view image of the RVN sums up the vascular networks and overlays the top vessels on the deep vessels. This may cause some of the deep vessels (i.e., capillary network) invisible, which may be the reason that the density of RVD was very close to SVD. In addition to the analysis of RVD and SVP, analyzing DVP may be crucial. A morphometric study showed that DVP has larger capillary density, smaller loop area, and vessel gap compared with SVP.[37] Using OCTA, recent studies revealed that DVP may be more vulnerable in diabetic retinopathy (DR) patients.[38–40] Bhanushali et al.[40] found that the spacing between vessels in DVP could be a better indicator of adverse vascular changes in DR. Couturier et al.[39] reported that in DR patients, the regular pattern of the capillary vortexes could not be identified in DVP and the number of the microaneurysms was significantly higher in DVP in comparison to SVP. Sambhav et al.[38] described that as DR progressed, a decrease in perfusion index was more pronounced in DVP, which preceded the vascular changes in SVP. It is worth noting that the vessel density in the annuli was smaller in DVP compared to RVN and SVP because there was a larger avascular zone in DVP compared that in RVN and SVP.

Retinal hemodynamics may play an important role in the onset and progression of age-related vascular pathogenesis in different types of retinopathies.[8,17,19,20] As a noninvasive imaging technique, RFI possesses several advantages for quantitative evaluation of the retinal microvascular hemodynamics.[41–43] In the present study, the mean velocities were calculated to be 3.55 mm/s in arterioles and 2.85 mm/s in venules by RFI, which are in agreement with previously reported studies by both our group[17] and others.[16,44] Interestingly, an increase of arteriolar BFV was observed in G3 group (50–65 years), while there was no significant drop of microvessel densities. The reduction of retinal arteriole calibre and arteriovenous ratio occurs during aging.[45] At the age more than 50 years old, the reduction reached more than

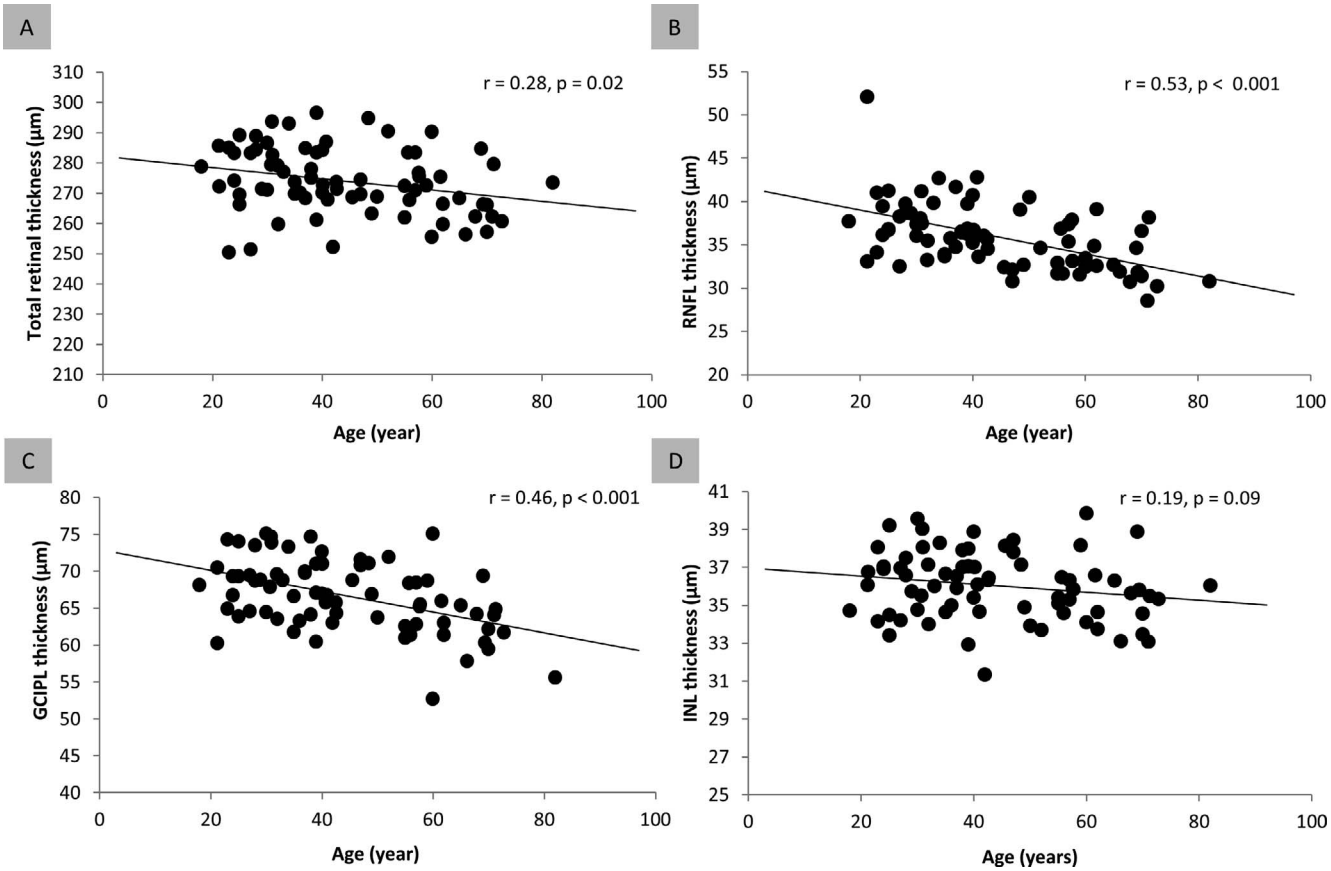

Figure 10. Relationship between age and the thicknesses of inner retinal layers. (**A**) Plot using the TRT. (**B**) Plot using the thickness of the RNFL. (**C**) Plot using the thickness of the GCIPL. (**D**) Plot using the thickness of the INL.

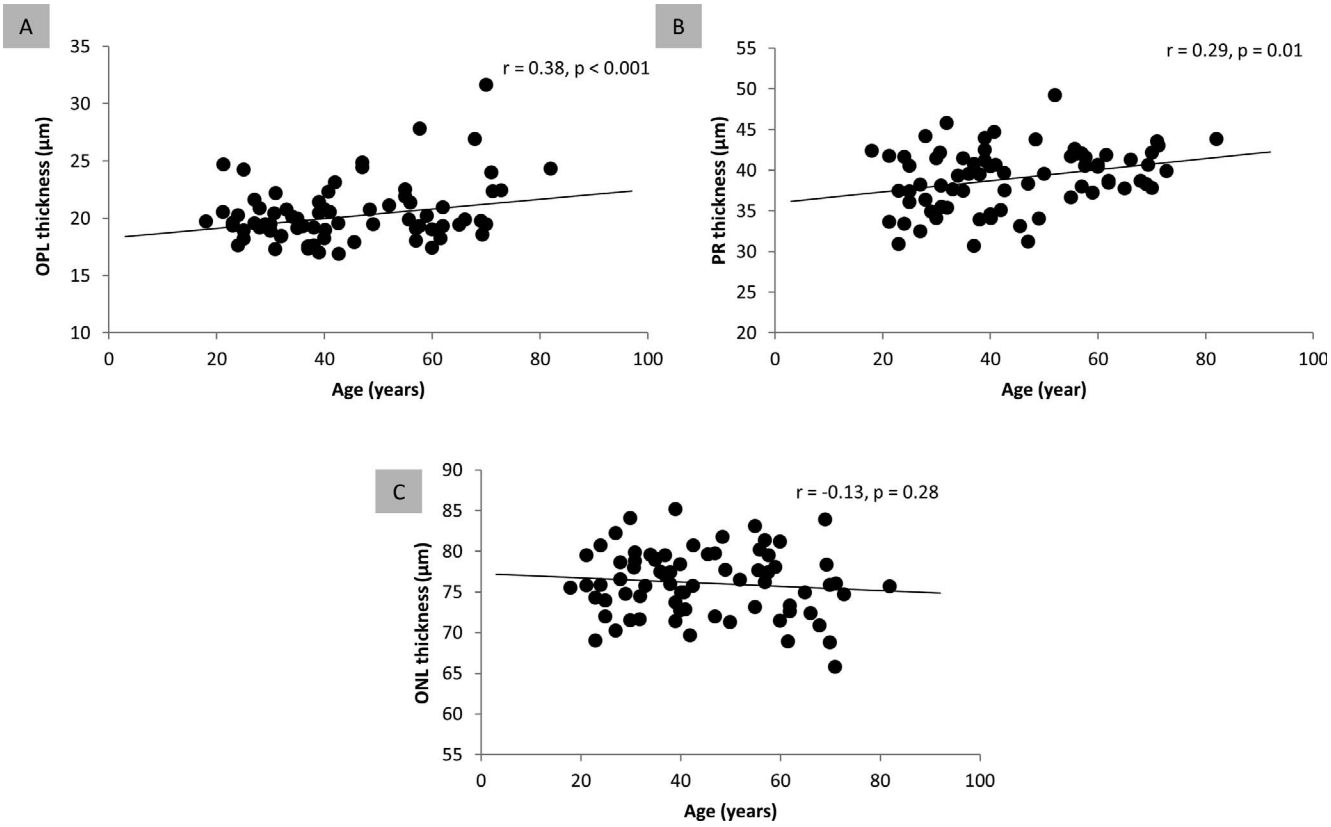

Figure 11. Relationship between age and the thicknesses of outer retinal layers. (**A**) Plot using the thicknesses of the OPL. (**B**) Plot using the thickness of the PR. (**C**) Plot using the thickness of the ONL.

Investigative Ophthalmology & Visual Science

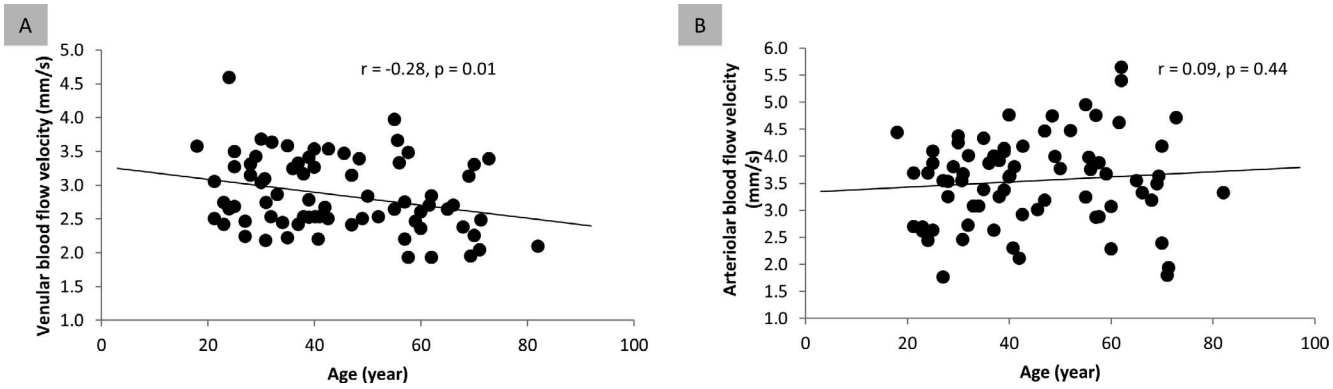

Figure 12. Relationship between age and retinal BFVs. (**A**) Venular BFV. (**B**) Arteriolar BFV.

50% of the all changes over the lifespan.[45] This phenomenon is supported by the measurement of retinal vessel wall using adaptive optics retinal camera, and age was associated with the increased wall-to-lumen ratio (WLR) of the retinal arterioles.[46] A significant increase of WLR was found in the middle age group (40–59 years), compared to young group (20–39 years). In the G3 group in the present study, there was no significant drop of the retinal vessel density, possibly indicating intact tissue perfusion. To maintain the needed perfusion level in the circumstance of narrowed arterioles, the increased BFV in the arterioles is expected. In contrast, G4 group had significant decreases of small vessel density and the thickness of the inner retinal layers, which may indicate less demand of tissue perfusion. This eventually ended up with the low blood flow volume, which may be the main reason of the decreased retinal venular BFV found in the present study.

A negative relation was found between age and retinal venular velocity, with a decrease of 3.5% per decade from 20 to 80 years. Previous results were reported by Burgansky-Eliash et al.,[8] who observed a reduction in venular velocity of 9.7% per decade above 40 years. One explanation for the age-associated decline in venous flow velocity in the retina is attributed to capillary loss during aging, leading to slower blood flow through the venules. In the present study, retinal micro-vessel loss was evident and related to venular velocity, which could explain the decreased venular velocity.

Aging causes alterations in all components of the neurovascular-hemodynamic system, whereas these components are theoretically interlinked. In a cross-sectional analysis such as in the present study, it is not possible to detect in which component these changes occur first. Future longitudinal studies will need to address the temporal nature of these changes. From our results, it could be speculated that the thinning of macular RNFL may happen first, as early as at 35 to 50 years of age. Clearly, after 65 years of age, changes in all components occur. Because the arteriole blood flow is adequately maintained by auto-regulation in normal aging, the alterations in the microcirculation may be delayed compared to the changes in retinal structure and vasculature. This difference may explain the decreased venular velocity that was evident only in the oldest group in our study.

The coincident effect of aging on the microstructure, microvasculature, and hemodynamics of the retina was demonstrated in the present study (Fig. 15). These unique data were essential as a baseline for further investigation on the pathogenesis and early diagnosis of retinopathies. Earlier studies only obtained preliminary data on the relation between retinal thickness and perfusion in the macula.[9] Analyzing microstructure, microvasculature, and hemodynamics in the same area of the same subject group with aging may provide a unique opportunity to establish the relations among these essential components in the vascular system of the retina.

Table 3. Correlations Between Age and Microstructure, Microvasculature, and Microcirculation

UHR-OCT	TRT	RNFL	GCIPL	INL	OPL	ONL	PR
Thickness, μm	275.4 ± 11.0	36.9 ± 3.9	67.8 ± 4.9	36.0 ± 1.8	20.4 ± 2.6	75.4 ± 4.1	38.8 ± 3.8
Relation, r	−0.28*	−0.53*	−0.46*	−0.19	0.38*	−0.13	0.29*
Change per year, %	−0.07	−0.35	−0.21	−0.06	0.20	−0.04	0.18
Change per decade, μm	−1.91	−1.29	−1.39	−0.21	0.42	−0.32	0.69
OCTA	3RVD	3SVD	3DVD	6RVD	6SVD	6DVD	
Vessel density, Dbox	1.758 ± 0.029	1.748 ± 0.032	1.734 ± 0.036	1.809 ± 0.022	1.797 ± 0.027	1.784 ± 0.046	
Relation, r	−0.40*	−0.31*	−0.43*	−0.35*	−0.29*	−0.28*	
Change per year, %	−0.039	−0.034	−0.058	−0.028	−0.028	−0.045	
Change per decade, Dbox	−0.007	−0.006	−0.01	−0.005	−0.005	−0.008	
RFI	Arteriole	Venule					
BFV, mm/s	3.55 ± 0.83	2.85 ± 0.54					
Relation, r	0.09	−0.28*					
Change per year, %	0.14	−0.35					
Change per decade, mm/s	0.05	−0.1					

Asterisk (*) denotes $P < 0.05$. 3RVD, retinal vessel density in the annulus from 0.6 to 2.5 mm; 3SVD, superficial vessel density in the annulus from 0.6 to 2.5 mm; 3DVD, deep vessel density in the annulus from 0.6 to 2.5 mm; 6RVD, retinal vessel density in the annulus from 0.6 to 5.0 mm; 6SVD, superficial vessel density in the annulus from 0.6 to 5.0 mm; 6DVD, deep vessel density in the annulus from 0.6 to 5.0 mm.

Investigative Ophthalmology & Visual Science

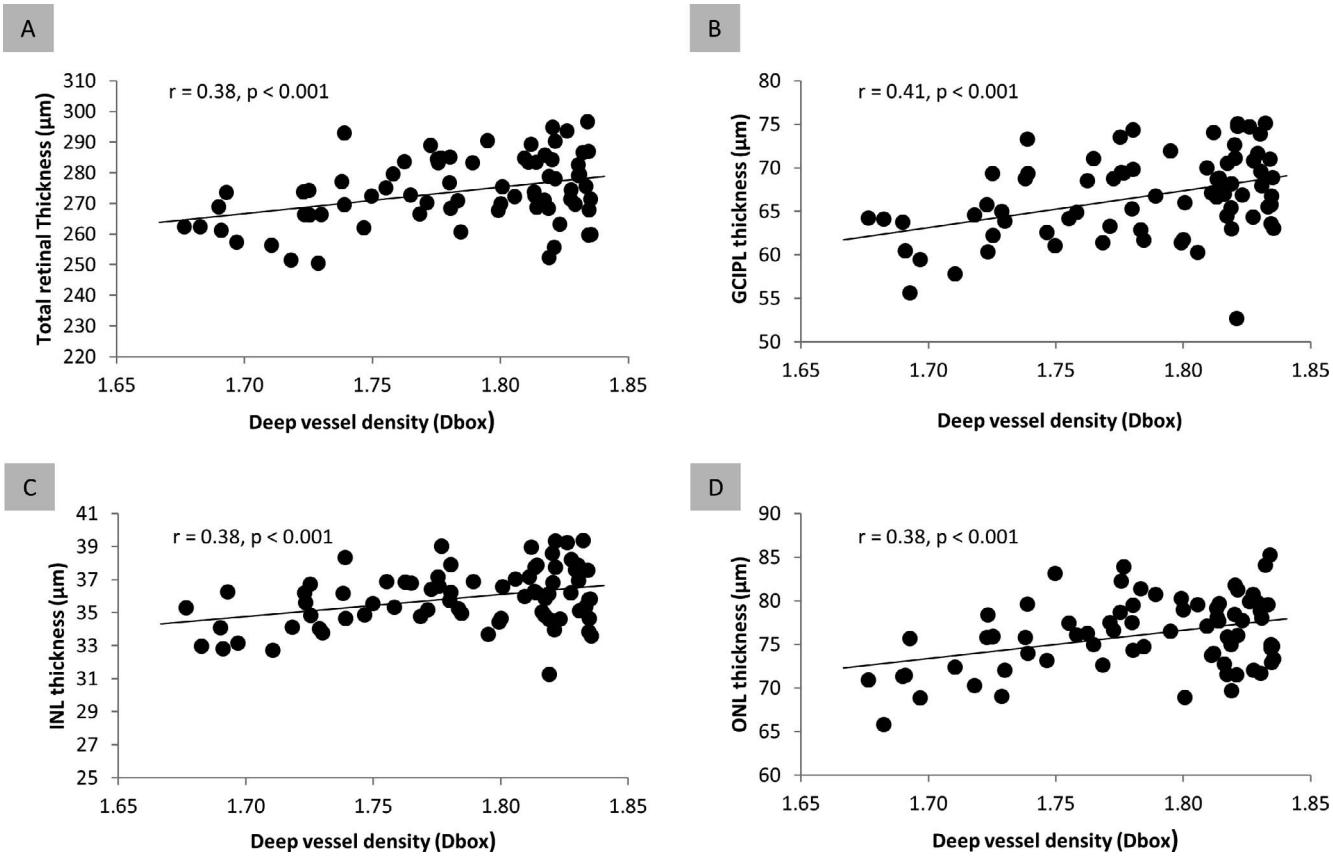

Figure 13. Relationship between deep vessel density and the thickness of retinal layers. (**A**) TRT. (**B**) GCIPL thickness. (**C**) INL thickness. (**D**) ONL thickness.

Based on detailed tomographic information of the inner and outer retina, we analyzed the relationship between the quantitative characteristics of the microstructure and retinal perfusion. Significantly, DVP density in the annulus from 0.6 to 5.0 mm was demonstrated to have strong correlations with TRT, GCL, INL, and ONL thickness in the perifoveal region. This interrelation was consistent with histological findings that showed that DVP is the microvascular network located between the INL and ONL. Additionally, such findings provided evidence to confirm the concurrent decline in blood perfusion and the neural structure of the retina with aging, which might be associated with the decrease in visual function in older populations. In the human retina, the superficial plexus contain arterioles, venules, and capillaries, whereas the DVP mainly consisted of capillary meshwork.[47] A morphometric study showed that the DVP has larger capillary density with smaller loop area and vessel gap compared with SVP.[37] These histological and morphological features of DVP might correspond to its vital role in the oxygen supply and metabolic process for the inner retina, which may further impact the inner retinal structure.

Perifoveal RNFL, GCIPL thickness, and venular BFV were observed to be negatively correlated with increasing age. However, no correlation was established between the BFV and thickness of any sublayers in the macula obtained from the same area. Similarly, Burgansky-Eliash et al.[8] reported a lack of correlation between BFV and peripapillary RNFL thickness or central macular thickness. As part of the cardiovascular system, retinal microcirculation was reported to be affected by systemic parameters in healthy subjects, such as heart rate, mean arterial pressure, and sex. By contrast, the relationship between retinal structure and retinal circulation becomes obvious in diseased conditions. A significant correlation was found between venular BFV and central retinal volume in patients with retinal diseases.[48] Sakata et al.[49] found that BFV was correlated with retinal thickness at the central fovea in patients with diabetic macular edema. In patients with early stage, open-angle glaucoma, Berisha et al.[50] showed that a thinner peripapillary RNFL was associated with a higher retinal blood flow measured by a laser Doppler blood flow instrument. These findings may indicate that the alteration in retinal microstructure and microcirculation occur under pathological conditions, which might offer diagnostic information for distinguishing patients with retinal pathologies from healthy aging subjects. Alternatively, the relationship between retinal structure and microcirculation may be speculated through the link between microcirculation and microvasculature (i.e., the vessel network).

This is the first study to report significant correlations between retinal vessel density and venular BFV, which revealed the inherent association of hemodynamics with microvasculature in the perifoveal region. During aging, the loss of the retinal capillary network was believed to lead to the decline of venular BFV. However, no correlation was identified between retinal vessel density and arteriolar BFV. Arteriolar BFV quantified by RFI corresponds to blood supply in secondary and tertiary branches of the central retinal vessels. These arteriolar retinal branches further form superficial and deep capillary networks, which are responsible for blood delivery to the inner retinal layers.[47] Autoregulation may be an explanation for the absence of age-

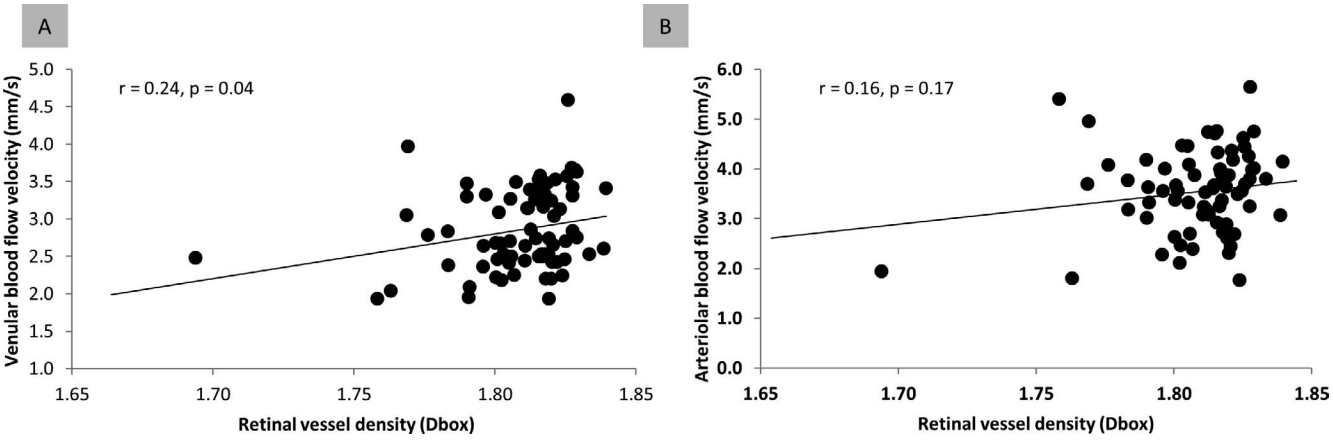

Figure 14. Relationship between retinal vessel density and retinal BFV. (**A**) Venular BFV. (**B**) Arteriolar BFV.

related coincidence between capillary network density and blood flow supply. These findings provide vital insights into the neuro-vascular-hemodynamic mechanism that supports the metabolic demands and homeostasis in the inner segment of the retina.

There are some limitations of the present study. First, although a relatively large sample was acquired with a wide range of ages, the sample size might still be small, and the oldest old subjects (age ≥85 years) may also need to be included. Further collection from more subjects may add more values to our database, which will be used as controls when patients with diseases are studied. Second, we did not perform a longitudinal study, which may reveal the order and temporal trends of these changes during aging. We used subgroups to study changes in an attempt to reveal age-related alterations, and used the whole group to establish the relations. Further longitudinal studies may further validate our findings. Third, the large vessels in SVP project the shadow on DVP, resulted in shadowgraphic project artifacts. The inherited algorithms did not remove the artifacts. Removing the shadowgraphic projection artifacts without accessing the inherited OCTA algorithm may lead to some degrees of inaccurate measurements of DVP. Nevertheless, the large vessels of DVP were removed using our custom image process software in the present study. The removal of the large vessel in DVP may reduce the shadowgraphic projection artifacts when fractal analysis of DVP was performed.[13] Finally, data acquired using OCTA and UHR-OCT were automatically processed, whereas data acquired using RFI were manually drawn then automatically processed. Manual selections of vessels may have measurement bias. Further development of automated processing may improve the measurements.

In summary, the present study presented age-related changes in retinal microvasculature, microcirculation, and microstructure and their interconnection in healthy subjects across a wide age range. During aging, decreases in retinal vessel density, inner retinal layer thickness, and venular BFV

Table 4. Summary of Age-Related Changes in Microstructure, Microvasculature, and Microcirculation

				Microstructure			
Reference	Eyes, *n*	Age, y	Microvasculature Vessel Density	RNFL Thickness	GCL Thickness	Outer Retina Thickness	Microcirculation Blood Flow
Present study	74 eyes 74 subjects	18–82	Related	Related	Related		Related (venule)
Yu et al.[9] 2016	121 eyes 64 subjects	20–62	Not related ($\beta = 0.000103$)				
Yu et al.[10] 2015	76 eyes 45 subjects	24–59	Related ($t = -6.103$)				
Gadde et al.[11] 2015	52 eyes	20–67	Not related				
Zhang et al.[26] 2016	192 eyes 92 subjects	40–75		Related	Related		
Kenmochi et al.[22] 2016	127 eyes 127 subjects	50–88				Related	
Demirkaya et al.[21] 2013	120 subjects	18–81		Related ($r = 0.332$)	Related ($r = 0.354$)	Related ($r = 0.381$)	
Koh et al.[25] 2012	623 subjects	40–80			Related ($\beta = -0.202$)		
Alamouti et al.[6] 2003	100 eyes 100 subjects	6–79		Related			
Gao et al.[29] 1992	35 donor eyes	17–95			Related	Related	
Burgansky-Eliash et al.[8] 2013	114 eyes 67 subjects	19–81					Related (venule)

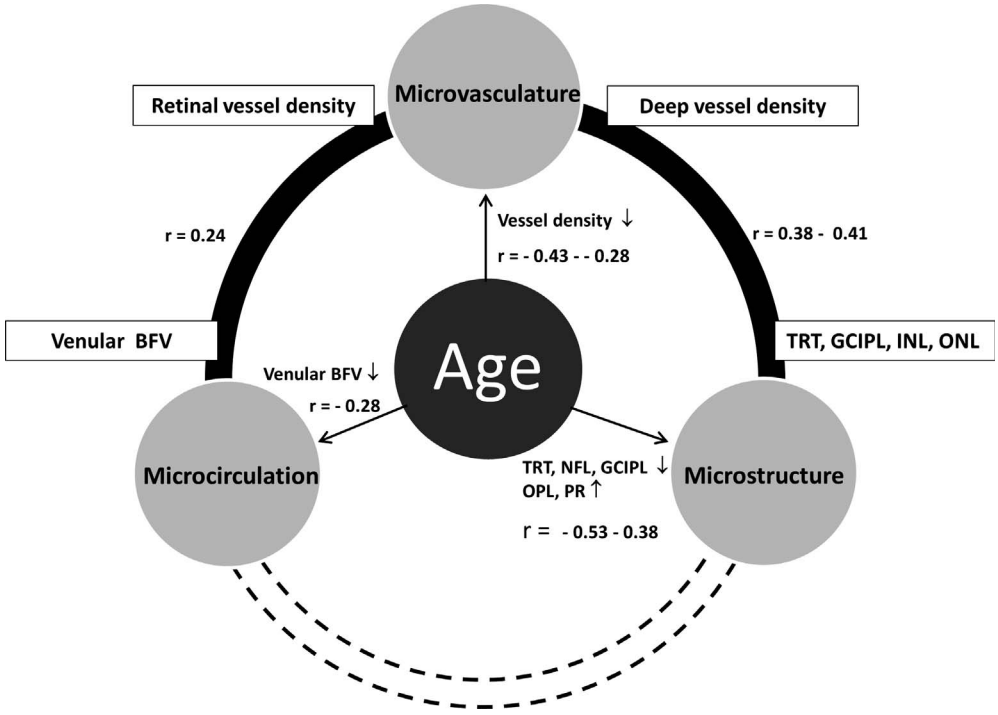

Figure 15. The age-related changes and interlink among retinal microstructure, microvasculature, and microcirculation. Overall, aging played a role in the thinning of the retinal inner segment, loss of retinal microvasculature, and decreased venular BFV. The changes in microvasculature were related to thinning of the inner retina and venular blood flow.

were evident and impacted each other as observed by simultaneous changes in multiple retinal components.

Acknowledgments

Supported by North American Neuro-ophthalmology Society, McKnight Brain Institute, National Institutes of Health Center Grant P30 EY014801, and a grant from Research to Prevent Blindness (RPB).

Disclosure: **Y. Wei**, None; **H. Jiang**, None; **Y. Shi**, None; **D. Qu**, None; **G. Gregori**, Carl Zeiss Meditec (F); **F. Zheng**, None; **T. Rundek**, None; **J. Wang**, None

References

1. Yu DY, Cringle SJ. Oxygen distribution and consumption within the retina in vascularised and avascular retinas and in animal models of retinal disease. *Prog Retin Eye Res*. 2001;20:175–208.
2. Jiang H, Delgado S, Liu C, et al. In vivo characterization of retinal microvascular network in multiple sclerosis. *Ophthalmology*. 2016;123:437–438.
3. Burgansky-Eliash Z, Nelson DA, Bar-Tal OP, et al. Reduced retinal blood flow velocity in diabetic retinopathy. *Retina*. 2010;30:765–773.
4. Guidoboni G, Harris A, Cassani S, et al. Intraocular pressure, blood pressure, and retinal blood flow autoregulation: a mathematical model to clarify their relationship and clinical relevance. *Invest Ophthalmol Vis Sci*. 2014;55:4105–4118.
5. Huang D, Swanson EA, Lin CP, et al. Optical coherence tomography. *Science*. 1991;254:1178–1181.
6. Alamouti B, Funk J. Retinal thickness decreases with age: an OCT study. *Br J Ophthalmol*. 2003;87:899–901.
7. Iverson SM, Feuer WJ, Shi W, Greenfield DS. Frequency of abnormal retinal nerve fibre layer and ganglion cell layer SDOCT scans in healthy eyes and glaucoma suspects in a prospective longitudinal study. *Br J Ophthalmol*. 2014;98:920–925.
8. Burgansky-Eliash Z, Lowenstein A, Neuderfer M, et al. The correlation between retinal blood flow velocity measured by the retinal function imager and various physiological parameters. *Ophthalmic Surg Lasers Imaging Retina*. 2013;44:51–58.
9. Yu J, Gu R, Zong Y, et al. Relationship between retinal perfusion and retinal thickness in healthy subjects: an optical coherence tomography angiography study. *Invest Ophthalmol Vis Sci*. 2016;57:OCT204–OCT210.
10. Yu J, Jiang C, Wang X, et al. Macular perfusion in healthy Chinese: an optical coherence tomography angiogram study. *Invest Ophthalmol Vis Sci*. 2015;56:3212–3217.
11. Gadde SG, Anegondi N, Bhanushali D, et al. Quantification of vessel density in retinal optical coherence tomography angiography images using local fractal dimension. *Invest Ophthalmol Vis Sci*. 2016;57:246–252.
12. Rosenfeld PJ, Durbin MK, Roisman L, et al. ZEISS angioplex spectral domain optical coherence tomography angiography: technical aspects. *Dev Ophthalmol*. 2016;56:18–29.
13. Yang Y, Wang J, Jiang H, et al. Retinal microvasculature alteration in high myopia. *Invest Ophthalmol Vis Sci*. 2016;57:6020–6030.
14. Li M, Yang Y, Jiang H, et al. Retinal microvascular network and microcirculation assessments in high myopia. *Am J Ophthalmol*. 2017;174:56–67.
15. Zhang M, Hwang TS, Campbell JP, et al. Projection-resolved optical coherence tomographic angiography. *Biomed Opt Express*. 2016;7:816–828.
16. Landa G, Jangi AA, Garcia PM, Rosen RB. Initial report of quantification of retinal blood flow velocity in normal human subjects using the Retinal Functional Imager (RFI). *Int Ophthalmol*. 2012;32:211–215.
17. Jiang H, Delgado S, Tan J, et al. Impaired retinal microcirculation in multiple sclerosis. *Mult Scler*. 2016;22:1812–1820.

18. Tan J, Yang Y, Jiang H, et al. The measurement repeatability using different partition methods of intraretinal tomographic thickness maps in healthy human subjects. *Clin Ophthalmol*. 2016;10:2403–2415.
19. Burgansky-Eliash Z, Barak A, Barash H, et al. Increased retinal blood flow velocity in patients with early diabetes mellitus. *Retina*. 2012;32:112–119.
20. Pournaras CJ, Rungger-Brandle E, Riva CE, Hardarson SH, Stefansson E. Regulation of retinal blood flow in health and disease. *Prog Retin Eye Res*. 2008;27:284–330.
21. Demirkaya N, van Dijk HW, van Schuppen SM, et al. Effect of age on individual retinal layer thickness in normal eyes as measured with spectral-domain optical coherence tomography. *Invest Ophthalmol Vis Sci*. 2013;54:4934–4940.
22. Kenmochi J, Ito Y, Terasaki H. Changes of outer retinal thickness with increasing age in normal eyes and in normal fellow eyes of patients with uilateral age-related macular degeneration. *Retina*. 2017;37:47–52.
23. Garas A, Vargha P, Hollo G. Diagnostic accuracy of nerve fibre layer, macular thickness and optic disc measurements made with the RTVue-100 optical coherence tomograph to detect glaucoma. *Eye (Lond)*. 2011;25:57–65.
24. Harwerth RS, Wheat JL. Modeling the effects of aging on retinal ganglion cell density and nerve fiber layer thickness. *Graefes Arch Clin Exp Ophthalmol*. 2008;246:305–314.
25. Koh VT, Tham YC, Cheung CY, et al. Determinants of ganglion cell-inner plexiform layer thickness measured by high-definition optical coherence tomography. *Invest Ophthalmol Vis Sci*. 2012;53:5853–5859.
26. Zhang X, Francis BA, Dastiridou A, et al. Longitudinal and cross-sectional analyses of age effects on retinal nerve fiber layer and ganglion cell complex thickness by fourier-Domain OCT. *Trans Vis Sci Tech*. 2016;5(2):1.
27. Da PS, Iacono P, Marchesan R, Minutola D, Ravalico G. The effect of ageing on retinal nerve fibre layer thickness: an evaluation by scanning laser polarimetry with variable corneal compensation. *Acta Ophthalmol Scand*. 2006;84:375–379.
28. Schlottmann PG, De CS, Greenfield DS, Caprioli J, Garway-Heath DF. Relationship between visual field sensitivity and retinal nerve fiber layer thickness as measured by scanning laser polarimetry. *Invest Ophthalmol Vis Sci*. 2004;45:1823–1829.
29. Gao H, Hollyfield JG. Aging of the human retina. Differential loss of neurons and retinal pigment epithelial cells. *Invest Ophthalmol Vis Sci*. 1992;33:1–17.
30. Ooto S, Hangai M, Tomidokoro A, et al. Effects of age, sex, and axial length on the three-dimensional profile of normal macular layer structures. *Invest Ophthalmol Vis Sci*. 2011;52:8769–8779.
31. Yu DY, Cringle SJ. Oxygen distribution in the mouse retina. *Invest Ophthalmol Vis Sci*. 2006;47:1109–1112.
32. Yu DY, Cringle SJ, Su EN. Intraretinal oxygen distribution in the monkey retina and the response to systemic hyperoxia. *Invest Ophthalmol Vis Sci*. 2005;46:4728–4733.
33. Maruko I, Arakawa H, Koizumi H, et al. Age-dependent morphologic alterations in the outer retinal and choroidal thicknesses using swept source optical coherence tomography. *PLoS One*. 2016;11:e0159439.
34. Karampelas M, Sim DA, Keane PA, et al. Evaluation of retinal pigment epithelium-Bruch's membrane complex thickness in dry age-related macular degeneration using optical coherence tomography. *Br J Ophthalmol*. 2013;97:1256–1261.
35. Okubo A, Rosa RH Jr, Bunce CV, et al. The relationships of age changes in retinal pigment epithelium and Bruch's membrane. *Invest Ophthalmol Vis Sci*. 1999;40:443–449.
36. Okubo A, Sameshima M, Unoki K, Uehara F, Bird AC. Ultrastructural changes associated with accumulation of inclusion bodies in rat retinal pigment epithelium. *Invest Ophthalmol Vis Sci*. 2000;41:4305–4312.
37. Chan G, Balaratnasingam C, Yu PK, et al. Quantitative morphometry of perifoveal capillary networks in the human retina. *Invest Ophthalmol Vis Sci*. 2012;53:5502–5514.
38. Sambhav K, Abu-Amero KK, Chalam KV. Deep capillary macular perfusion indices obtained with OCT angiography correlate with degree of nonproliferative diabetic retinopathy [published online ahead of print March 27, 2017]. *Eur J Ophthalmol*. doi:10.5301/ejo.5000948.
39. Couturier A, Mane V, Bonnin S, et al. Capillary plexus anomalies in diabetic retinopathy on optical coherence tomography. *Retina*. 2015;35:2384–2391.
40. Bhanushali D, Anegondi N, Gadde SG, et al. Linking retinal microvasculature features with severity of diabetic retinopathy using optical coherence tomography angiography. *Invest Ophthalmol Vis Sci*. 2016;57:OCT519–OCT525.
41. Burgansky-Eliash Z, Bartov E, Barak A, Grinvald A, Gaton D. Blood-flow velocity in glaucoma patients measured with the Retinal Function Imager. *Curr Eye Res*. 2016;41:965–970.
42. Feng X, Kedhar S, Bhoomibunchoo C. Retinal blood flow velocity in patients with active uveitis using the retinal function imager. *Chin Med J (Engl)*. 2013;126:1944–1947.
43. Landa G, Rosen RB. A new vascular pattern for idiopathic juxtafoveal telangiectasia revealed by the retinal function imager. *Ophthalmic Surg Lasers Imaging*. 2010;41:413–417.
44. Ganekal S. Retinal functional imager (RFI): non-invasive functional imaging of the retina. *Nepal J Ophthalmol*. 2013;5:250–257.
45. Pose-Reino A, Gomez-Ulla F, Hayik B, et al. Computerized measurement of retinal blood vessel calibre: description, validation and use to determine the influence of ageing and hypertension. *J Hypertens*. 2005;23:843–850.
46. Meixner E, Michelson G. Measurement of retinal wall-to-lumen ratio by adaptive optics retinal camera: a clinical research. *Graefes Arch Clin Exp Ophthalmol*. 2015;253:1985–1995.
47. Foreman DM, Bagley S, Moore J, et al. Three dimensional analysis of the retinal vasculature using immunofluorescent staining and confocal laser scanning microscopy. *Br J Ophthalmol*. 1996;80:246–251.
48. Landa G, Garcia PM, Rosen RB. Correlation between retina blood flow velocity assessed by retinal function imager and retina thickness estimated by scanning laser ophthalmoscopy/optical coherence tomography. *Ophthalmologica*. 2009;223:155–161.
49. Sakata K, Funatsu H, Harino S, Noma H, Hori S. Relationship of macular microcirculation and retinal thickness with visual acuity in diabetic macular edema. *Ophthalmology*. 2007;114:2061–2069.
50. Berisha F, Feke GT, Hirose T, McMeel JW, Pasquale LR. Retinal blood flow and nerve fiber layer measurements in early-stage open-angle glaucoma. *Am J Ophthalmol*. 2008;146:466–472.

Investigative Ophthalmology & Visual Science